

We are IntechOpen, the world's leading publisher of Open Access books Built by scientists, for scientists

6,900

Open access books available

185,000

International authors and editors

200M

Downloads

Our authors are among the

154

Countries delivered to

TOP 1%

most cited scientists

12.2%

Contributors from top 500 universities



WEB OF SCIENCE™

Selection of our books indexed in the Book Citation Index
in Web of Science™ Core Collection (BKCI)

Interested in publishing with us?
Contact book.department@intechopen.com

Numbers displayed above are based on latest data collected.
For more information visit www.intechopen.com



Variants of Kalman Filter for the Synchronization of Chaotic Systems

Sadasivan Puthusserypady¹ and Ajeesh P. Kurian²

¹*Department of Electrical and Computer Engineering, National University of Singapore*

²*Department of Electrical and Computer Engineering, University of Calgary*

¹*Singapore*

²*Canada*

1. Introduction

Perhaps the most important lesson to be drawn from the study of nonlinear dynamical systems over the past few decades is that even simple dynamical systems can give rise to complex behaviour which is statistically indistinguishable from that produced by a complex random process. Chaotic systems are nonlinear systems which exhibit such complex behaviour. In such systems, the state variables move in a bounded, aperiodic, random-like fashion. A distinct property of chaotic dynamics is its long-term unpredictability. In such systems, initial states which are very close to each other produce markedly different trajectories. When nearby points evolve to result in uncorrelated trajectories, while forming the same attractor, the dynamical system is said to possess sensitive dependence to initial conditions (Devaney, 1985). Due to these desirable properties, application of chaotic systems are explored for many engineering applications such as secure communications, data encryption, digital water marking, pseudo random number generation etc (Kennedy et. al., 2000). In most of these applications, it is essential to synchronize the chaotic systems at two different locations. In this chapter, we explore the Kalman filter based chaotic synchronization.

2. Synchronization of chaotic systems

Related works of synchronization dates back to the research carried out by Fujisaka and Yamada in 1983 (Fujisaka & Yamada, 1983). Pecora and Carroll suggested a drive-response system for synchronization of chaotic systems. They showed that if all the transversal Lyapunov exponents of the response system are negative, the systems synchronize asymptotically (Pecora & Carrol, 1990). Later a plethora of research work was reported on synchronization of chaotic systems (Nijmeijer & Mareels, 1997). One of the well researched approaches is the coupled synchronization, where a proper coupling is introduced between the transmitter and the receiver. The chaotic systems synchronize asymptotically when the coupling strength is above a certain threshold, which is determined by the local Lyapunov exponents (Suchichik et. al., 1997).

Let the transmitter and the receiver states of the chaotic systems be given by

Source: Kalman Filter, Book edited by: Vedran Kordić,
ISBN 978-953-307-094-0, pp. 390, May 2010, INTECH, Croatia, downloaded from SCIYO.COM

$$\mathbf{x}_{k+1} = \mathbf{f}(\mathbf{x}_k, \mu) \quad (1.a)$$

$$\hat{\mathbf{x}}_{k+1} = \mathbf{f}(\hat{\mathbf{x}}_k, \hat{\mu}) \quad (1.b)$$

where $\mathbf{x}_k = [x_k^1, \dots, x_k^n]^T$ and $\hat{\mathbf{x}}_k = [\hat{x}_k^1, \dots, \hat{x}_k^n]^T$ are the n -dimensional state vectors of the transmitter and the receiver systems, respectively. μ and $\hat{\mu}$ are the transmitter and the receiver system parameters and $\mathbf{f} = [f^1(\cdot), \dots, f^n(\cdot)]^T$ is a smooth nonlinear vector valued function. Normally, we have a noisy observation at the receiver which is given by

$$\mathbf{y}_k = \mathbf{h}(\mathbf{x}_k) + \mathbf{v}_k \quad (2)$$

where \mathbf{v}_k is the channel noise and $\mathbf{h}(\cdot)$ is the measurement function. These two systems are said to be synchronized if

$$\lim_{k \rightarrow \infty} \|\mathbf{x}_k - \hat{\mathbf{x}}_k\| = 0. \quad (3)$$

2.1 Coupled synchronization

In coupled synchronization, a coupling is introduced between the transmitter and the receiver as:

$$\hat{\mathbf{x}}_k = \mathbf{f}(\hat{\mathbf{x}}_{k-1}) + \mathbf{K}_k(\mathbf{y}_k - \hat{\mathbf{y}}_k) \quad (4)$$

where \mathbf{K}_k is the appropriate coupling coefficient matrix. In conventional coupled synchronization, \mathbf{K}_k is set to be a constant value such that the global and local Lyapunov exponents (The Lyapunov exponents of a dynamic system are the quantities that characterize the rate of divergence/convergence of the trajectories generated by infinitesimally close initial conditions under the dynamics) are negative. This makes the receiver to synchronize with the transmitter asymptotically. The schematic of the coupled synchronization is shown in Fig. 1. This method of synchronization can be treated as a predictor corrector filter approach. In general, a predictive filter predicts the subsequent states and corrects it with additional information available from the observation. Due to the measurement and the channel noises in a communication system, stochastic techniques have to be applied for synchronization. Instead of keeping \mathbf{K}_k as a constant value if it is determined adaptively, the coupled synchronization has a similarity with the predictive filtering techniques.

3. Chaos synchronization: a stochastic estimation view point

In stochastic state estimation methods, one would like to estimate the state variable \mathbf{x}_k based on the set of all available (noisy) measurement $\mathbf{y}_{1:k} = \{\mathbf{y}_1, \dots, \mathbf{y}_k\}$ with certain degree of confidence. This is done by constructing the conditional probability density function (pdf), $p(\mathbf{x}_k | \mathbf{y}_{1:k})$ (i.e. the probability of \mathbf{x}_k given the observations, $\mathbf{y}_{1:k}$), known as the posterior probability. It is assumed that $p(\mathbf{x}_0 | \mathbf{y}_0)$ is available. In predictor corrector filtering methods, $p(\mathbf{x}_k | \mathbf{y}_{1:k})$ is obtained recursively by a prediction step which is estimated without the knowledge of current measurement, \mathbf{y}_k followed by a correction step where the knowledge of \mathbf{y}_k is used to make the correction to the predicted values.

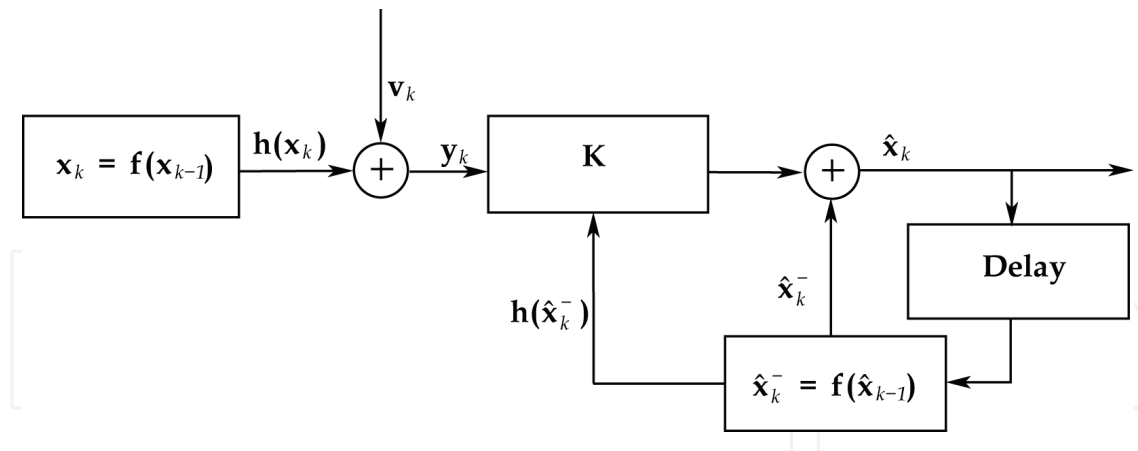


Fig. 1. Schematic of the coupled synchronization scheme.

In the recursive computation of $p(\mathbf{x}_k | \mathbf{y}_{1:k})$, it is assumed that at time, $k - 1$, $p(\mathbf{x}_{k-1} | \mathbf{y}_{1:k-1})$ is available. Using the Chapman-Kolmogorov equation (Arulampalam, et. al. 2001), the prediction is estimated as

$$p(\mathbf{x}_k | \mathbf{y}_{1:k-1}) = \int p(\mathbf{x}_k | \mathbf{x}_{k-1})p(\mathbf{x}_{k-1} | \mathbf{y}_{1:k-1})d\mathbf{x}_{k-1} \tag{5}$$

where the state transition is assumed to be a Markov process of order one and $p(\mathbf{x}_k | \mathbf{x}_{k-1}, \mathbf{y}_{1:k-1}) = p(\mathbf{x}_k | \mathbf{x}_{k-1})$. To make the correction, one needs to make use of the information available in the current observation, \mathbf{y}_k . Using Bayes' rule,

$$p(\mathbf{x}_k | \mathbf{y}_{1:k}) = \frac{p(\mathbf{x}_k | \mathbf{y}_{1:k-1})p(\mathbf{y}_k | \mathbf{x}_k)}{p(\mathbf{y}_k | \mathbf{y}_{1:k-1})} \tag{6}$$

where the normalizing constant

$$p(\mathbf{y}_k | \mathbf{y}_{1:k-1}) = \int p(\mathbf{y}_k | \mathbf{x}_k)p(\mathbf{x}_k | \mathbf{y}_{1:k-1})d\mathbf{x}_k \tag{7}$$

Though closed form solutions of the above equations exist for a linear system with Gaussian noise (e.g. Kalman filter), in general, for a nonlinear system, they are not available. However, one of the suboptimal filtering methods, the extended Kalman filter (EKF) is found to be useful in many nonlinear filtering applications.

3.1 EKF for chaos synchronization

The Kalman filter is an optimal recursive estimation algorithm for linear systems with Gaussian noise. A distinctive feature of this filter is that its mathematical formulation is described in terms of the state-space. The EKF is an extension of the Kalman filtering algorithm to nonlinear systems (Grewal & Andrews, 2001). The system is linearized using first order Taylor series approximation. To this approximated system, the Kalman filter is applied to obtain the state estimates. Consider a generic dynamic system governed by

$$\mathbf{x}_k = \mathbf{f}(\mathbf{x}_{k-1}, \mathbf{w}_k) \tag{8.a}$$

$$\mathbf{y}_k = \mathbf{h}(\mathbf{x}_k, \mathbf{v}_k) \tag{8.b}$$

where the process noise, \mathbf{w}_k , and observation (measurement) noise, \mathbf{v}_k , are zero mean Gaussian processes with covariance matrices \mathbf{Q}_k and \mathbf{R}_k , respectively. In minimum mean square estimation (MMSE), the receiver computes $\hat{\mathbf{x}}_k$ which is an estimate of \mathbf{x}_k from the available observations $\mathbf{y}_{1:k} = \{\mathbf{y}_1, \dots, \mathbf{y}_k\}$ such that the mean square error (MSE), $\mathbb{E}[\mathbf{e}_k^T \mathbf{e}_k]$ (where $\mathbf{e}_k = \mathbf{x}_k - \hat{\mathbf{x}}_k$), is minimized. The EKF algorithm for the state estimation is given by,

$$\hat{\mathbf{x}}_{k|k-1} = \mathbf{f}(\hat{\mathbf{x}}_{k-1}, 0), \quad (9.a)$$

$$\mathbf{P}_{k|k-1} = \mathbf{F}_{k-1} \mathbf{P}_{k-1} \mathbf{F}_{k-1}^T + \mathbf{W}_k \mathbf{Q}_k \mathbf{W}_k^T \quad (9.b)$$

In the above equations, the notation $k|k-1$ denotes an operation performed at time instant, k , using the information available till $k-1$. At time instant k , $\hat{\mathbf{x}}_{k|k-1}$ is the *a priori* estimate of the state vector \mathbf{x}_k , $\mathbf{P}_{k|k-1}$ is the *a priori* error covariance matrix, \mathbf{F}_{k-1} is the Jacobian of $\mathbf{f}(\cdot)$ with respect to the state vector \mathbf{x}_{k-1} and \mathbf{W}_k is the Jacobian of $\mathbf{f}(\cdot)$ with respect to the noise vector \mathbf{w}_k . The EKF update equations are:

$$\mathbf{K}_k = \mathbf{P}_{k|k-1} \mathbf{H}_k^T \left\{ \mathbf{H}_k \mathbf{P}_{k|k-1} \mathbf{H}_k^T + \mathbf{V}_k \mathbf{R}_k \mathbf{V}_k^T \right\}^{-1} \quad (10.a)$$

$$\hat{\mathbf{x}}_k = \hat{\mathbf{x}}_{k|k-1} + \mathbf{K}_k (\mathbf{y}_k - \hat{\mathbf{y}}_k) \quad (10.b)$$

$$\mathbf{P}_k = (\mathbf{I} - \mathbf{K}_k \mathbf{H}_k) \mathbf{P}_{k|k-1} \quad (10.c)$$

where \mathbf{K}_k is the Kalman gain, \mathbf{H}_k is the Jacobian of $\mathbf{h}(\cdot)$ with respect to $\hat{\mathbf{x}}_{k|k-1}$, $\hat{\mathbf{x}}_k$ is the *a posteriori* estimate of the state vector, \mathbf{V}_k is the Jacobian of $\mathbf{h}(\cdot)$ with respect to the noise vector \mathbf{v}_k , and \mathbf{P}_k is the *a posteriori* error covariance matrix. When EKF is used for synchronization of chaotic maps, \mathbf{K}_k acts as the coupling strength which is updated iteratively. Schematic of EKF based synchronization is shown in Fig. 2.

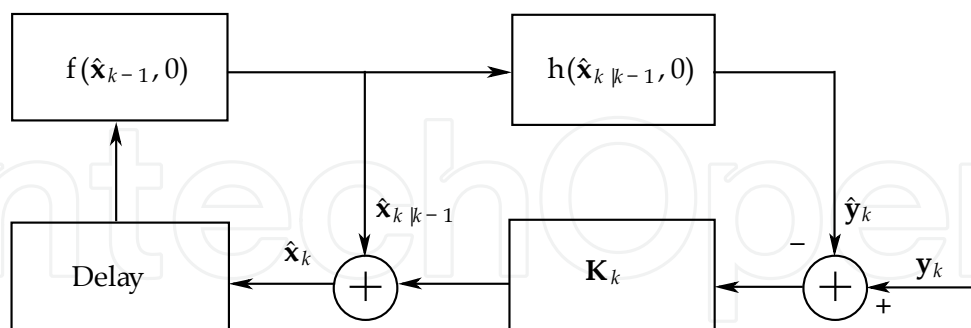


Fig. 2. Schematic of EKF based chaos synchronization

3.2.1 Convergence analysis

Convergence analysis of \mathbf{K}_k can be carried out by studying the convergence of $\mathbf{P}_{k|k-1}$. At any time instant, k , according to the *matrix fraction propagation* of $\mathbf{P}_{k|k-1}$, it can be shown that (Grewal & Andrews, 2001),

$$\mathbf{P}_{k|k-1} = \mathbf{A}_k \mathbf{B}_k^{-1}, \quad (11)$$

where \mathbf{A}_k and \mathbf{B}_k^{-1} are factors of $\mathbf{P}_{k|k-1}$. If \mathbf{F}_k is nonsingular (i.e. the map is invertible), then \mathbf{A}_{k+1} and \mathbf{B}_{k+1} are given by the recursive equation as

$$\begin{bmatrix} \mathbf{A}_{k+1} \\ \mathbf{B}_{k+1} \end{bmatrix} = \begin{bmatrix} \mathbf{F}_k + \mathbf{W}_k \mathbf{F}_k^{-T} \mathbf{H}_k^T \mathbf{R}_k^{-1} \mathbf{H}_k & \mathbf{W}_k \mathbf{F}_k^{-T} \\ \mathbf{F}_k^{-T} \mathbf{H}_k^T \mathbf{R}_k^{-1} \mathbf{H}_k & \mathbf{F}_k^{-T} \end{bmatrix} \begin{bmatrix} \mathbf{A}_k \\ \mathbf{B}_k \end{bmatrix}. \quad (12)$$

From the above expression, it can be shown that, when there is no process noise (i.e. $\mathbf{W}_k = \mathbf{0}$ and \mathbf{F}_k is *contractive* (i.e. the magnitudes of its eigenvalues are less than one), $\mathbf{P}_{k|k-1}$ will converge in time. However, inside the chaotic attractor, the behaviour of $\mathbf{P}_{k|k-1}$ is aperiodic if \mathbf{F}_k is time varying. This behaviour has dramatic influence on the convergence of Kalman filter based synchronization system (Kurian, 2006) for systems with hyperbolic tangencies (HTs).

3.3 Unscented Kalman filter

The approximation error introduced by the EKF together with the expansions of this error at the HTs makes the system unstable and diverging trajectories are generated at the receiver. One way to mitigate this problem is to use nonlinear filters with better approximation capabilities. Unscented Kalman filter (UKF) has shown to possess these capabilities (Julier & Uhlman, 2004). It is essentially an approximation method to solve Eq. (5). UKF works based on the principle of unscented transform (UT) (Julier & Uhlman, 1997).

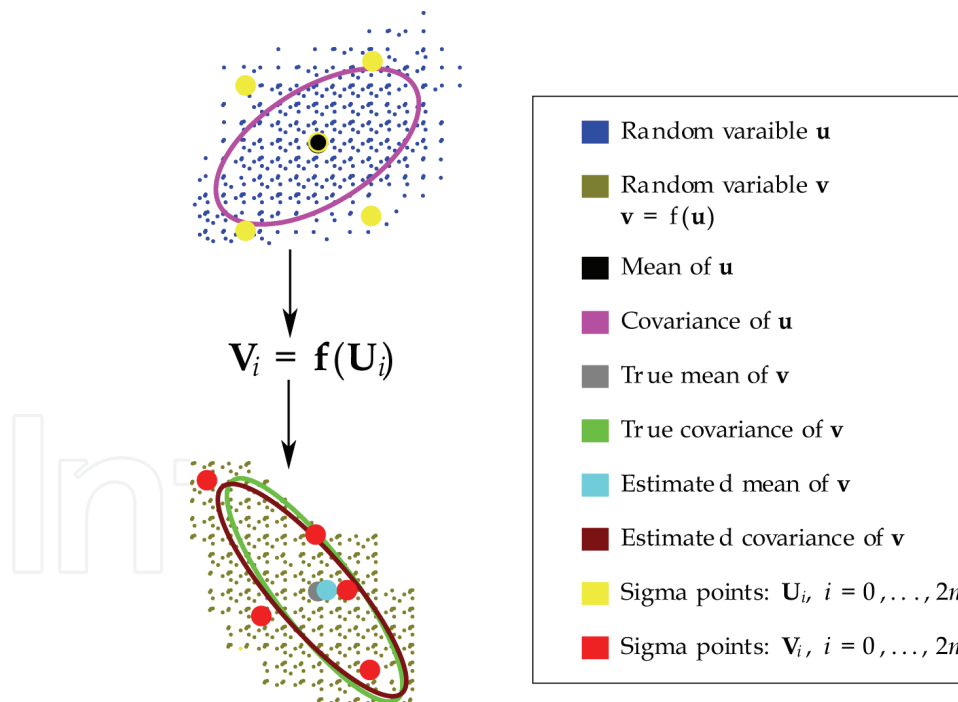


Fig. 3. Illustration of unscented transform (UT).

In Fig. 3, the UT of a random variable, \mathbf{u} , which undergoes a nonlinear transformation ($\mathbf{f}(\mathbf{u})$) to result in another random variable, \mathbf{v} is shown. To calculate the statistics of \mathbf{v} , the ideal solution is to get posterior density, $p(\mathbf{v})$, analytically from the prior density $p(\mathbf{u})$. The mean and covariance of \mathbf{v} can also be computed analytically. However, this is highly impractical in most of the situations because of the nonlinearity. UT is a method for

approximating the statistics of a random variable which undergoes a nonlinear transformation. It uses carefully selected vectors (\mathcal{U}_i), known as *sigma points*, to approximate the statistics of the posterior density. Each sigma point is associated with a weight W_i . The number of sigma points is $2n+1$ where n is the dimension of the state vector. With the knowledge of the mean ($\hat{\mathbf{u}}$) and covariance (\mathbf{P}_u) of the prior density, these sigma points are constructed as

$$\begin{aligned} (\mathcal{U}_0, W_0) &= \left(\hat{\mathbf{u}}, \frac{\kappa}{n+\kappa} \right); & i=0 \\ (\mathcal{U}_i, W_i) &= \left(\hat{\mathbf{u}} + \left(\sqrt{(n+\kappa)\mathbf{P}_u} \right)_i, \frac{1}{2(n+\kappa)} \right); & i=1, \dots, n \\ (\mathcal{U}_i, W_i) &= \left(\hat{\mathbf{u}} - \left(\sqrt{(n+\kappa)\mathbf{P}_u} \right)_i, \frac{1}{2(n+\kappa)} \right); & i=n+1, \dots, 2n \end{aligned} \quad (13)$$

where κ is a scaling parameter and $\left(\sqrt{(n+\kappa)\mathbf{P}_u} \right)_i$ is the i th row or column of the square root of the matrix, $(n+\kappa)\mathbf{P}_u$. These sigma points are propagated through the nonlinearity $\mathbf{f}(\cdot)$ to obtain

$$\mathcal{V}_i = \mathbf{f}(\mathcal{U}_i) \quad \text{for } i=0, 1, \dots, 2n. \quad (14)$$

Using the set of \mathcal{V}_i , the mean ($\hat{\mathbf{v}}$) and covariance (\mathbf{P}_v) of the posterior density is estimated as

$$\hat{\mathbf{v}} = \sum_{i=0}^{2n} W_i \mathcal{V}_i \quad (15.a)$$

$$\mathbf{P}_v = \sum_{i=0}^{2n} W_i (\mathcal{V}_i - \hat{\mathbf{v}})(\mathcal{V}_i - \hat{\mathbf{v}})^T. \quad (15.b)$$

It is shown that the UKF based approximation is equivalent to a third order Taylor series approximation if the Gaussian prior is assumed (Julier & Uhlman, 2004). Another advantage of UT is that it does not require the calculation of the Jacobian or Hessian.

3.3.1 Scaled unscented transform

The scaled unscented transform (SUT) is a generalization of the UT. It is a method that scales an arbitrary set of sigma points yet capture the mean and covariance correctly. The new transform is given by

$$\mathcal{U}'_i = \mathcal{U}_0 + \alpha(\mathcal{U}_i - \mathcal{U}_0) \quad \text{for } i=0, \dots, 2n \quad (16)$$

where α is a positive scaling parameter. By this the distribution of the sigma points can be controlled without affecting the positive definitive nature of the matrix, $(n+\kappa)\mathbf{P}_u$. A set of sigma points, $\{\mathbf{U} = [\mathcal{U}_0, \dots, \mathcal{U}_{2n}], \mathbf{W} = [W_0, \dots, W_{2n}]\}$, is first calculated using Eq.(13) and then transformed into scaled sigma points, $\{\mathbf{U}' = [\mathcal{U}'_0, \dots, \mathcal{U}'_{2n}], \mathbf{W}' = [W'_0, \dots, W'_{2n}]\}$ by

$$\mathcal{U}'_i = \mathcal{U}_0 + \alpha(\mathcal{U}_i - \mathcal{U}_0) \quad \text{for } i = 0, 1, \dots, 2n \quad (17.a)$$

$$W'_i = \begin{cases} \frac{W_0}{\alpha^2} + (1 - \frac{1}{\alpha^2}) & i = 0 \\ \frac{W_i}{\alpha^2} & i \neq 0 \end{cases} \quad (17.b)$$

The sigma point selection and scaling can be combined to a single step by setting

$$\lambda = \alpha^2(n + \kappa) - n \quad (18)$$

and

$$\mathcal{U}'_0 = \hat{\mathbf{u}} \quad (19.a)$$

$$\mathcal{U}'_i = \hat{\mathbf{u}} + (\sqrt{(n + \lambda)\mathbf{P}_u})_i \quad i = 1, \dots, n \quad (19.b)$$

$$\mathcal{U}'_i = \hat{\mathbf{u}} - (\sqrt{(n + \lambda)\mathbf{P}_u})_i \quad i = n + 1, \dots, 2n \quad (19.c)$$

$$W_0^{(m)} = \frac{\lambda}{n + \lambda} \quad (19.d)$$

$$W_0^{(c)} = \frac{\lambda}{(n + \lambda)} + (1 - \alpha^2 + \beta) \quad (19.e)$$

$$W_i^{(m)} = W_i^{(c)} = \frac{1}{2(\lambda + n)} \quad \text{for } i = 1, 2, \dots, 2n. \quad (19.f)$$

Parameter β above is another control parameter which affects the weighting of the zeroth sigma point for the calculation of the covariance. Using SUT, the mean and the covariance can be estimated as

$$\hat{\mathbf{v}} = \sum_{i=0}^{2n} W_i^{(m)} \mathcal{V}'_i \quad (20.a)$$

$$\mathbf{P}_v = \sum_{i=0}^{2n} W_i^{(c)} (\mathcal{V}'_i - \hat{\mathbf{v}})(\mathcal{V}'_i - \hat{\mathbf{v}})^T \quad (20.b)$$

where $\mathcal{V}'_i = \mathbf{f}(\mathcal{U}'_i)$.

Selection of κ is such that it should result in positive semi definiteness of the covariance matrix. $\kappa \geq 0$ guarantees this condition and a good choice is $\kappa = 0$. Choose $0 \leq \alpha \leq 1$ and $\beta \geq 0$. For Gaussian prior density, $\beta = 2$ is an optimal choice. Since, α controls the spread of the sigma points, it is selected such that it should not capture the non-local effects when nonlinearities are strong.

3.3.2 Unscented Kalman filter

UKF is an application of the SUT. It implements the minimum mean square estimates as follows. The objective is to estimate the states \mathbf{x}_k , given the observations, $\mathbf{y}_{1:k}$. For this, the state variable is redefined as the concatenation of the original state and noise variables (i.e. $\mathbf{x}_k^a = [\mathbf{x}_k^T \mathbf{w}_k^T \mathbf{v}_k^T]^T$ with dimension n_a). The steps involved in UKF are listed below. First, we initialize the parameters

$$\hat{\mathbf{x}}_0 = \mathbb{E}[\mathbf{x}_0] \quad (21.a)$$

$$\mathbf{P}_0 = \mathbb{E}[(\mathbf{x}_0 - \hat{\mathbf{x}}_0)(\mathbf{x}_0 - \hat{\mathbf{x}}_0)^T] \quad (21.b)$$

$$\hat{\mathbf{x}}_0^a = [\hat{\mathbf{x}}_0^T \mathbf{0} \mathbf{0}]^T \quad (21.c)$$

$$\mathbf{P}_0^a = \begin{bmatrix} \mathbf{P}_0 & \mathbf{0} & \mathbf{0} \\ \mathbf{0} & \mathbf{Q} & \mathbf{0} \\ \mathbf{0} & \mathbf{0} & \mathbf{R} \end{bmatrix} \quad (21.d)$$

For $k = 1, 2, \dots$ calculate the sigma points:

$$\mathcal{X}_{k-1}^a = \left[\hat{\mathbf{x}}_{k-1}^a \quad \hat{\mathbf{x}}_{k-1}^a \pm \sqrt{(n_a + \lambda)\mathbf{P}_{k-1}^a} \right] \quad (22)$$

Time update:

$$\mathcal{X}_{k|k-1} = \mathbf{f}(\mathcal{X}_{k-1}^x, \mathcal{X}_{k-1}^w) \quad (23.a)$$

$$\hat{\mathbf{x}}_{k|k-1} = \sum_{i=0}^{2n_a} W_i^{(m)} \mathcal{X}_{i,k|k-1}^x \quad (23.b)$$

$$\mathbf{P}_{k|k-1} = \sum_{i=0}^{2n_a} W_i^{(c)} [\mathcal{X}_{i,k|k-1}^x - \hat{\mathbf{x}}_{k|k-1}] [\mathcal{X}_{i,k|k-1}^x - \hat{\mathbf{x}}_{k|k-1}]^T \quad (23.c)$$

$$\mathcal{Y}_{k|k-1} = \mathbf{h}(\mathcal{X}_{k|k-1}^x, \mathcal{X}_{k|k-1}^v) \quad (23.d)$$

$$\hat{\mathbf{y}}_{k|k-1} = \sum_{i=0}^{2n_a} W_i^{(m)} \mathcal{Y}_{i,k|k-1} \quad (23.e)$$

Measurement update:

$$\mathbf{P}_{\hat{\mathbf{y}}_k \hat{\mathbf{y}}_k} = \sum_{i=0}^{2n_a} W_i^{(c)} [\mathcal{Y}_{i,k|k-1} - \hat{\mathbf{y}}_{k|k-1}] [\mathcal{Y}_{i,k|k-1} - \hat{\mathbf{y}}_{k|k-1}]^T \quad (24.a)$$

$$\mathbf{P}_{\hat{\mathbf{x}}_k \hat{\mathbf{y}}_k} = \sum_{i=0}^{2n_a} W_i^{(c)} [\mathcal{X}_{i,k|k-1}^x - \hat{\mathbf{x}}_{k|k-1}] [\mathcal{Y}_{i,k|k-1} - \hat{\mathbf{y}}_{k|k-1}]^T \quad (24.b)$$

$$\mathbf{K}_k = \mathbf{P}_{\hat{\mathbf{x}}_k \hat{\mathbf{y}}_k} \mathbf{P}_{\hat{\mathbf{y}}_k \hat{\mathbf{y}}_k}^{-1} \quad (24.c)$$

$$\hat{\mathbf{x}}_k = \hat{\mathbf{x}}_{k|k-1} + \mathbf{K}_k (\mathbf{y}_k - \hat{\mathbf{y}}_{k|k-1}) \quad (24.d)$$

$$\mathbf{P}_k = \mathbf{P}_{k|k-1} - \mathbf{K}_k \mathbf{P}_{\hat{\mathbf{y}}_k \hat{\mathbf{y}}_k} \mathbf{K}_k^T \quad (24.e)$$

It is shown in (Julier & Uhlman, 2004) that the approximation introduced by the UKF has more number of Taylor series terms. The effect of the approximation errors is different for different nonlinear systems. In some cases, if the nonlinearity is quadratic, approximation error will not have any strong influence.

4. Results and discussion

To assess the performance of the EKF and UKF based synchronization schemes, simulation studies are carried out on three different chaotic systems/maps¹: (i) Ikeda map (IM), (ii) Lorenz system, and (iii) Mackey-Glass (MG) system. The Lorenz system is a three dimensional vector field, $\phi(x, y, z): R^3 \rightarrow R^3$, representing the interrelation of temperature variation and convective motion. The set of coupled differential equations representing the Lorenz system is given by

$$\dot{x}(t) = \sigma(y(t) - x(t)) \quad (25.a)$$

$$\dot{y}(t) = -x(t)z(t) + rx(t) - y(t) \quad (25.b)$$

$$\dot{z}(t) = x(t)y(t) - cz(t) \quad (25.c)$$

where $\sigma = 10$, $r = 28$ and $c = 8/3$ are used to obtain the Lorenz attractor. The three states (x, y and z) are randomly initialized and the system of differential equation is solved with the fourth order Runge-Kutta method. The Lorenz attractor is shown in Fig. 4.

Ikeda map represent a discrete dynamic system of pumped laser beam around a lossy ring cavity and is defined as

$$z_{k+1} = p + Bz_k \exp \left[\sqrt{-1} \left(\phi - \frac{\omega}{1 + |z_k|^2} \right) \right] \quad (26)$$

where z_k is a complex-valued state variable with $z_k = x_k^R + \sqrt{-1}x_k^I$. Here, x_k^R is $\Re\{z_k\}$ and x_k^I is $\Im\{z_k\}$. $\Re\{\cdot\}$ and $\Im\{\cdot\}$ give the real and imaginary parts of a complex variable, respectively.

For the set of parameters $p = 0.92$, $B = 0.9$, $\phi = 0.4$, and $\omega = 6$, the attractor of this map is shown in Fig. 5.

The Mackey-Glass system was originally proposed as a first order nonlinear delay differential equation to describe physiological control systems. It is given by

¹ Map is used to represent discrete dynamic systems. i.e. $f: X \rightarrow X$

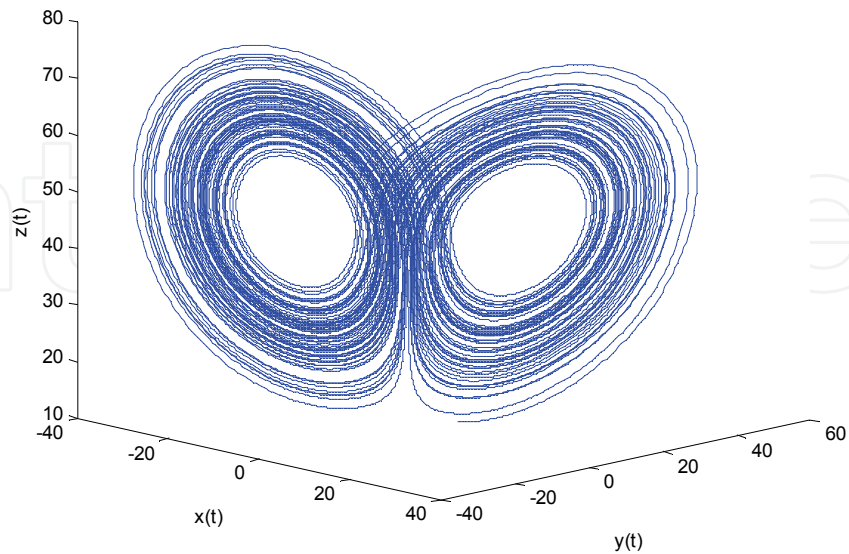


Fig. 4. Lorenz attractor.

$$\dot{x}(t) = -ax(t) + \frac{bx(t-\tau)}{1+x(t-\tau)^{10}} \quad (27)$$

This system is chaotic for values of $a=0.1$ and $\tau \geq 17$. Figure 6 shows the Mackey-Glass attractor with $\tau=17$.

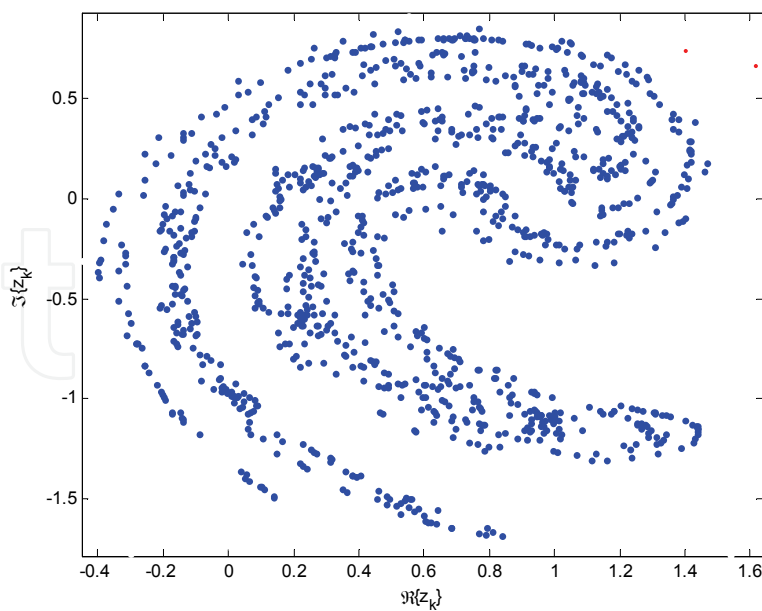


Fig. 5. Ikeda map attractor.

These systems/maps have distinct dynamical properties and well suited for our analysis. Lorenz system is one of the archetypical chaotic systems commonly studied for chaotic

synchronization. Ikeda map, on the other hand, has higher order derivatives and is an appropriate candidate for studying the effect of high nonlinearity in filter based synchronization. An interesting feature of Mackey-Glass system is that its complexity (i.e. the correlation dimension) increases as τ increases.

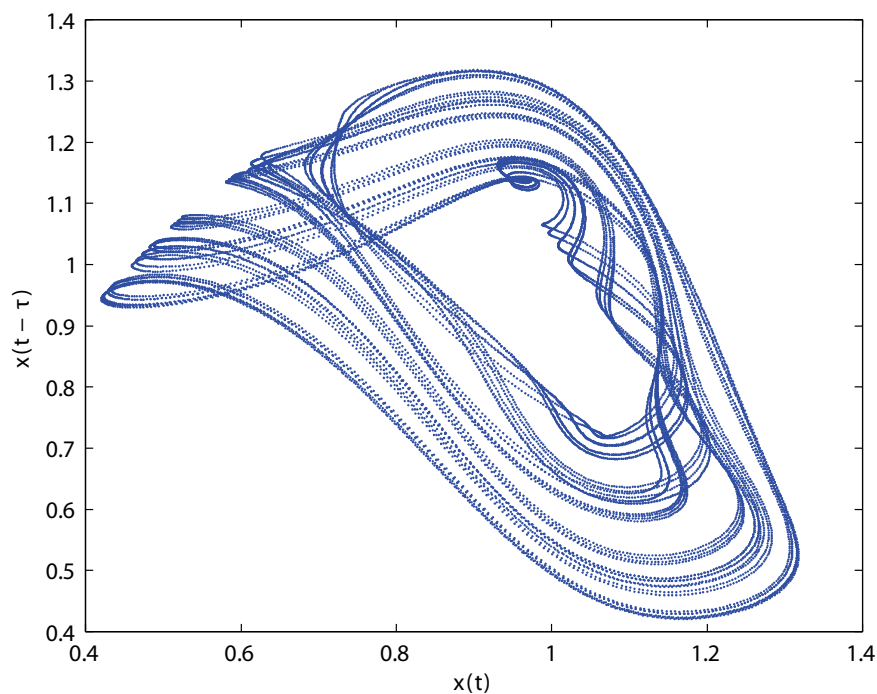


Fig. 6. Mackey-Glass Attractor.

We consider a typical situation where one of the state variables, x_k (for continuous system, it is assumed that we discretize the state variable using appropriate techniques) which is corrupted by channel noise is used for the synchronization. In all the computer simulations, the signal-to-noise ratio (SNR) which is defined as

$$\text{SNR} = \frac{1}{N} \sum_{k=1}^N x_k^2 \quad (28)$$

where σ_w^2 is the variance of the noise and N is the total number of samples used for evaluation, is varied from -5dB to 50dB for the Lorenz and MG systems and in the case of IM, it is varied from 35dB to 60dB. We define two performance evaluation quantities: the normalized mean square error (NMSE) and the total normalized mean square error (TNMSE) as

$$\text{NMSE}^i = \frac{\sum_{k=1}^N (x_k^i - \hat{x}_k^i)^2}{\sum_{k=1}^N (x_k^i)^2}, \quad (29)$$

$$\text{TNMSE} = \sum_{i=1}^n \text{NMSE}^i, \quad (30)$$

respectively. While NMSE gives an idea about the recovery of observed state variable, TNMSE gives how faithfully, the attractor can be reconstructed.

We run numerical simulations on all these three systems and the results are presented here. Figures 7 to 9 show the result of NMSE performances. We restricted the SNR from 35dB to 60dB in the case of IM system due to the observed divergence when both EKF and UKF are used. It is shown in (Kurian, 2006) that since the IM has non-hyperbolic chaotic attractors, this divergence is inevitable. For all other systems, we changed the SNR from -5dB to 50dB. We can see that for all the maps and systems we considered for the analysis, the NMSE is monotonically decreasing with the increase in SNR. The steady decrease in NMSE shows that there are no residual errors. Also, we can see that the UKF based synchronization gives very good NMSE performance due to the better approximation capabilities of the UKF. In the case of MG system, we can see that the EKF nearly fails in synchronizing at all SNRs which is again due to higher approximation error.

We computed the TNMSE values for the Lorenz system and Ikeda Map (Fig. 10 & 11). As mentioned before, the TNMSE values indirectly reflect how well the chaotic attractors could be reconstructed. The TNMSE values for Lorenz systems and Ikeda Map are always greater than the NMSE values at all the SNR values considered due to the error introduced by other state variables. We can see that this increase in error is comparable and behaves exactly like the NMSE: it gradually reduces with an increase in the SNR values. Similarly, the UKF shows better performance for all the SNR values considered.

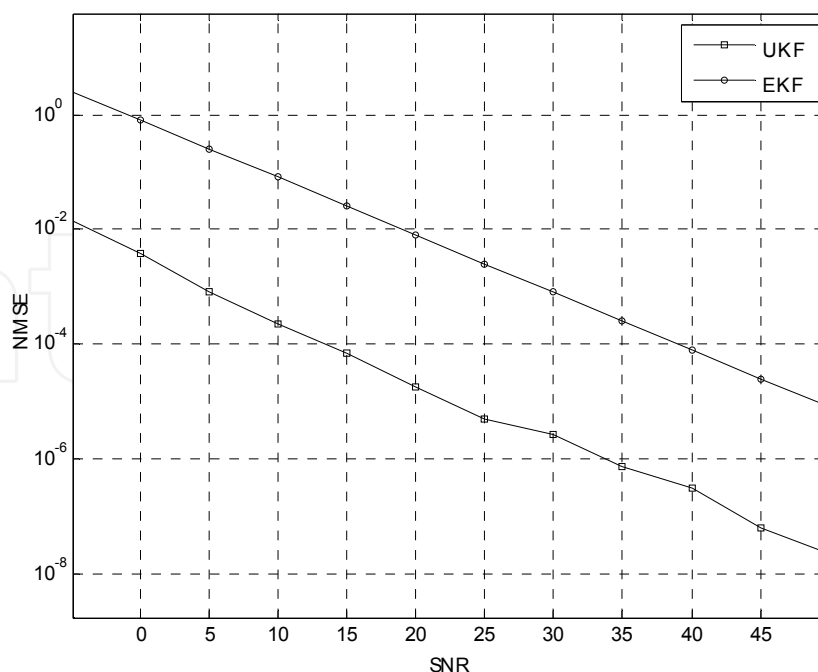


Fig. 7. NMSE of UKF and EKF based synchronization schemes for Lorenz.

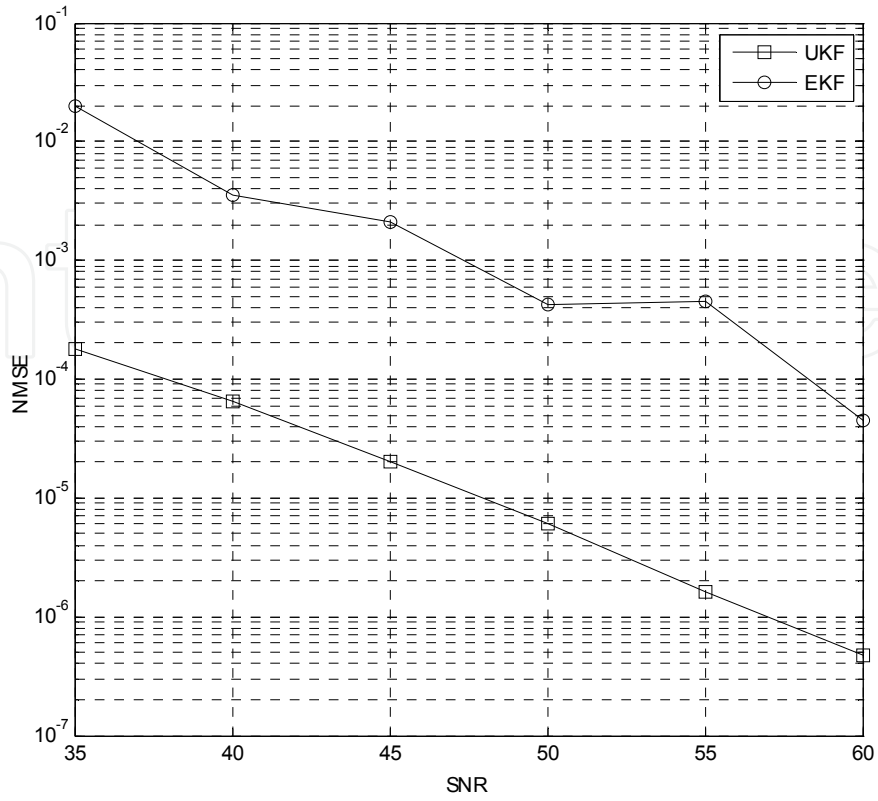


Fig. 8. NMSE of UKF and EKF based synchronization schemes for Ikeda map.

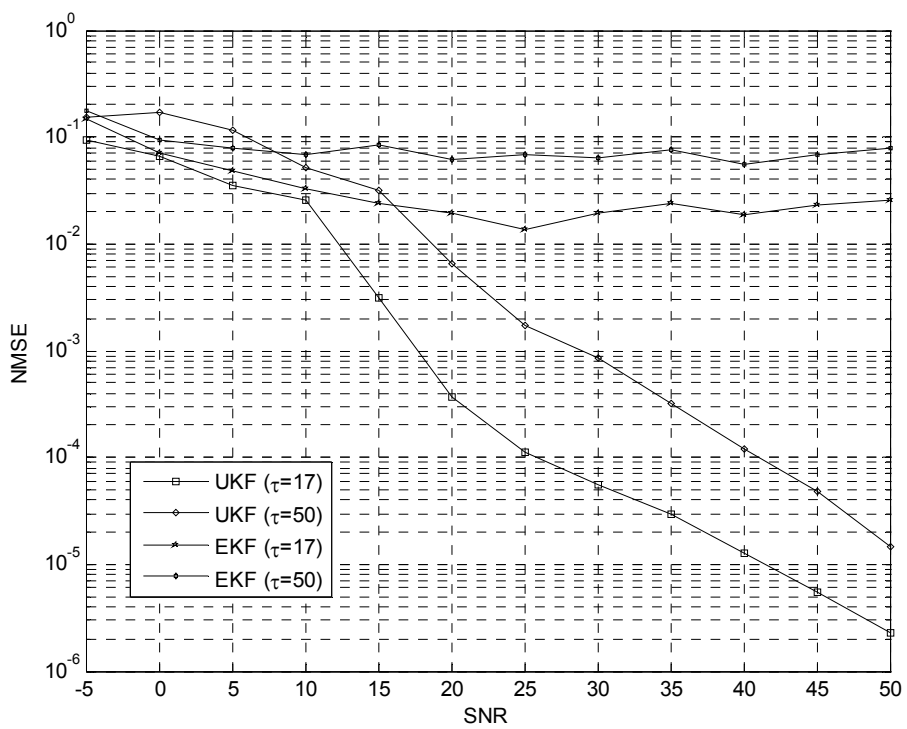


Fig. 9. NMSE of UKF and EKF based synchronization schemes for MG systems.

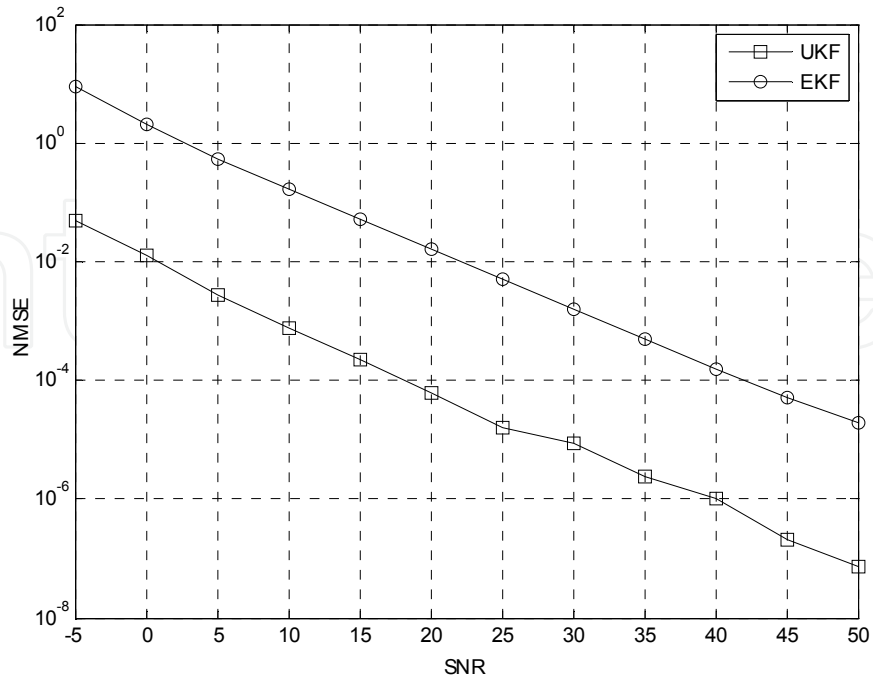


Fig. 10. TNMSE of UKF and EKF based synchronization schemes for Lorenz system.

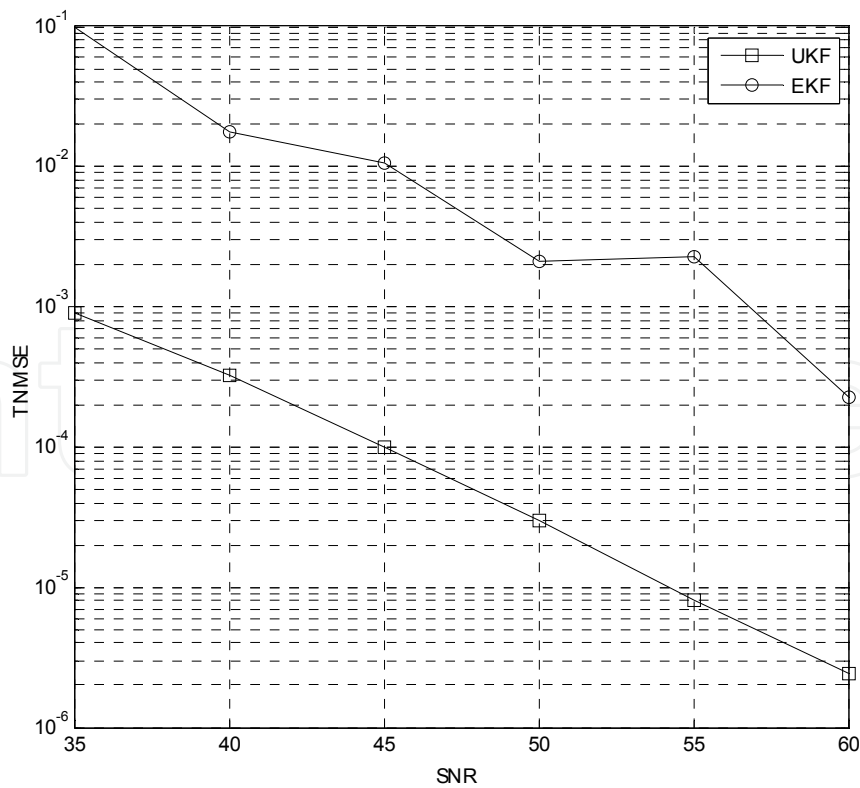


Fig. 11. TNMSE of UKF and EKF based synchronization schemes for Ikeda map.

5. Conclusions

Chaotic systems are simple dynamic systems which can display very complex behavior. One of the defining characteristics of such systems is the sensitive dependence on initial conditions and hence synchronization of such systems possesses certain amount of difficulties. This task will be even more formidable when the channels as well as the measurement noises are present in the system. Stochastic methods are applied to synchronize such chaotic systems. EKF is one of the most widely investigated stochastic filtering methods for chaotic synchronization. However, for highly nonlinear systems, EKF introduces approximation errors causing unacceptable degradation in the system performance. We consider UKF, which has better approximation error characteristics for chaos synchronization and show that it has better error characteristics.

6. References

- R. L. Devaney (1985). *An introduction to chaotic dynamical system*. The Benjamin Cummings Publishing Company Inc.
- M. P. Kennedy, R. Rovatti, and G. Setti (2000). *Chaotic electronics in telecommunications*. CRC Press.
- Fujisaka, H. & Yamada (1983). Stability theory of synchronized motion in coupled oscillator systems. *Progressive Theory of Physics*. Vol. 69, No. 1, pp. 32–47.
- Pecora, L. M. & Carroll, T. L. (1990). Synchronization in chaotic systems. *Physical Review Letters*. Vol. 64, pp. 821–824.
- Ogorzalek, M. J. (1993). Taming chaos–Part I: Synchronization. *IEEE Trans. Circuits Syst.–I*. vol. 40, No. 10, pp. 693–699.
- Sushchik, M. M.; Rulkov, N. F. & Abarbanel H. D. I. (1997). Robustness and stability of synchronized chaos: An illustrative model. *IEEE Trans. Circuits Syst.–I*, vol. 44, pp. 867–873.
- Nijmeijer, H. & Mareels, I. M. Y. (1997). An observer looks at synchronization. *IEEE Trans. Circuits Sys.–I*, vol. 44, No. 10, pp. 882–890.
- Arulampalam, S.; Maskell, S. ; Gordon, N. & Clapp, T. (2001). A tutorial on particle filters for on-line non-linear/non-Gaussian Bayesian tracking. *IEEE Trans. Signal Process.*, vol. 50, pp. 174–188.
- Grewal, M. S. & Andrews A. P. (2001). *Kalman filtering: Theory and practice using MATLAB*, 2nd Ed., John Wiley & Sons.
- Kurian, A. (2006). *Performance analysis of filtering based chaotic synchronization and development of chaotic digital communication schemes*. PhD Dissertation, National University of Singapore.
- Julier, S. J. & Uhlman, J. K. (2004). Unscented Kalman filtering and nonlinear estimation. *Proc. IEEE*, vol. 92, pp. 401–421.
- Eric, A. W. & van der Merwe, R. (2000). The unscented Kalman filter for nonlinear estimation, *Proc. IEEE Symposium on Adaptive Systems for Signal Processing, Communication and Control (AS-SPCC)*. Lake Louise, Alberta, Canada, Octobre.

Julier, S. J. & Uhlmann, J. K. (1997). A new extension of the Kalman filter to nonlinear systems. *Proc. of AeroSense: The 11th International Symposium on Aerospace/Defense Sensing, Simulation and Control*.

H. D. I. Abarbanel, *Analysis of observed chaotic data*. Springer, USA, 1996.

IntechOpen

IntechOpen



Kalman Filter

Edited by Vedran Kordic

ISBN 978-953-307-094-0

Hard cover, 390 pages

Publisher InTech

Published online 01, May, 2010

Published in print edition May, 2010

The Kalman filter has been successfully employed in diverse areas of study over the last 50 years and the chapters in this book review its recent applications. The editors hope the selected works will be useful to readers, contributing to future developments and improvements of this filtering technique. The aim of this book is to provide an overview of recent developments in Kalman filter theory and their applications in engineering and science. The book is divided into 20 chapters corresponding to recent advances in the field.

How to reference

In order to correctly reference this scholarly work, feel free to copy and paste the following:

Sadasivan Puthusserypady and Ajeesh P. Kurian (2010). Variants of Kalman Filter for the Synchronization of Chaotic Systems, Kalman Filter, Vedran Kordic (Ed.), ISBN: 978-953-307-094-0, InTech, Available from: <http://www.intechopen.com/books/kalman-filter/variants-of-kalman-filter-for-the-synchronization-of-chaotic-systems>

INTECH
open science | open minds

InTech Europe

University Campus STeP Ri
Slavka Krautzeka 83/A
51000 Rijeka, Croatia
Phone: +385 (51) 770 447
Fax: +385 (51) 686 166
www.intechopen.com

InTech China

Unit 405, Office Block, Hotel Equatorial Shanghai
No.65, Yan An Road (West), Shanghai, 200040, China
中国上海市延安西路65号上海国际贵都大饭店办公楼405单元
Phone: +86-21-62489820
Fax: +86-21-62489821

© 2010 The Author(s). Licensee IntechOpen. This chapter is distributed under the terms of the [Creative Commons Attribution-NonCommercial-ShareAlike-3.0 License](#), which permits use, distribution and reproduction for non-commercial purposes, provided the original is properly cited and derivative works building on this content are distributed under the same license.

IntechOpen

IntechOpen